

LUND UNIVERSITY

DEPARTMENT OF PHYSICS

DIVISION OF PARTICLE PHYSICS

BACHELOR THESIS

**Studying the sensitivity of the ATLAS
mono(H-bb) + missing transverse
momentum search for a Dark Higgs
signal**

Author:
David Madsen

Supervisor:
Ruth Pöttgen

April 23, 2018



LUND UNIVERSITY

Abstract

Dark Matter is one of the biggest mysteries in physics of our time, with an overwhelming amount of evidence for its existence but lack of direct observation (at time of writing). The focus of this thesis is to reimplement an ATLAS analysis used for Dark Matter searches in the mono- $H(b\bar{b})$ channel, and use that analysis in order to study the signal of a new particle called Dark Higgs. The Dark Higgs comes from assuming that Dark Matter particles acquire their mass in the same manner as Standard Model particles i.e via a Higgs mechanism in the dark sector. The signal samples used for this analysis are generated with a Monte Carlo simulation at truth level. The analysis was implemented in Rivet version 2.5.4 and the results produced show that even without dedicated optimization, the analysis exhibits a certain sensitivity, however there is lots of room for improvement.

Populärvetenskaplig artikel

Mörk materia är ett av de största nutida mysterier inom fysik och astronomi. Anledning till detta är för att det finns många tydliga tecken på att mörk materia existerar, men det har aldrig blivit direkt observerat.

Det man har observerat genom att bland annat studera galaxernas rotations hastighet är att det fattas materia för att galaxerna ska hålla ihop. Därav kom fysiker på konceptet mörk materia, vilket är materia vi inte kan se men är där ändå. Beräkningar visar att det finns ungefär 5 gånger mer mörk materia än vanlig materia i vårt universum! faktum är att enbart 5% av universum består av vanlig materia och ungefär 26 % är mörk materia. Resterande är något som kallas mörk energi.

En av de delarna inom fysiken som fokuserar mycket på att försöka observera mörk materia är partikelfysiken. Där kolliderar man partiklar med varandra i otroliga hastigheter i ett försök att skapa mörk materia partiklar. LHC (Large Hadron Collider) i Genève, Schweiz, är ett av de ställena där man gör dessa typer av kollisioner. På LHC kolliderar man två protoner som färdas i nästan ljusets hastighet med varandra, för att försöka skapa mörk materia partiklar.

Eftersom mörk materia partiklar inte interagerar med de detektorer som finns, så är det väldigt svårt att hitta dessa partiklar. Därför letar man efter den energi som fattas ifrån kollisionerna, denna energi kan tyda på att det har skapats mörk materia partiklar.

Mitt kandidat arbete har fokuserat på att implementera en ATLAS (experiment på LHC) analys där Higgs boson används för att söka efter mörk materia partiklar. Men istället för att använda Higgs boson så har vi använt simulationer för en ny partikel som kallas mörka Higgs boson. Det tros att den mörka Higgs bosonen är den mörka versionen av Higgs boson. Anledningen till att man tror att denna partikel finns, är för man antar att de mörka partiklarna får sin massa genom att interagera med ett mörkt Higgs fält, precis som de vanliga partiklar får sin massa genom att interagera med det vanliga Higgs fältet.

Eftersom vi har inte har någon aning om huruvida den mörka Higgs bosonen finns eller ej så har mitt kandidatarbete utgått ifrån att analysera ett antal simulerade partikel kollisioner. I dessa kollisioner bestämmer man den nya partikelns egenskaper och studerar hur effektiv analysen.

För att göra det lite mer begripligt så kan vi använda en analogi. Tänk dig att du har en boll vars egenskaper du vet om, nu kastar du iväg bollen och ska sedan försöka hitta den. För att kunna hitta bollen ingen så kan du välja att leta efter den på olika sätt. Genom att till exempel leta efter dess färger eller storlek. Därefter kan du kolla vilken metod som är bäst för att hitta bollen.

Det är ungefär det mitt kandidatarbete har handlat om. Vi har simulerat kollisioner där det skapas en mörk Higgs boson, och studerat ett av de många sätten att försöka hitta denna mörka Higgs boson. Nu kan man ju fråga sig vad detta är bra för, och varför man ska lägga tid på det? Anledningen till varför är egentligen ganska simpel, simulationerna som vi gör lägger grunden för att man kunna se ska vilket sätt som är det bästa sättet att leta efter den mörka Higgs bosonen. För ju fler sätt vi har att leta efter mörk materia partiklar desto större är chansen att man upptäcker det.

Contents

1	Introduction	4
2	Theory and Motivation	4
2.1	Standard Model	4
2.2	Higgs	6
2.2.1	Brout-Englert-Higgs mechanism	6
2.2.2	The Brout-Englert-Higgs field	6
2.2.3	Higgs Boson	7
2.3	Beyond the Standard Model	8
2.3.1	Dark Matter	8
2.3.2	Dark Higgs	9
3	LHC	10
4	ATLAS	11
5	Analysis	12
5.1	Jets	13
5.2	Selection cuts	13
5.3	b-tagging	15
5.4	Signal-sample	15
6	Results	16
7	Conclusion	25
8	Outlook	26
9	Acknowledgements	27
A	Analysis code	29
B	Additional figures	30

1 Introduction

For quite some time physicists have known that visible matter only makes up approximately 5% of the universe, while Dark Matter makes up approximately 26% and the rest being dark energy [1]. Due to the nature of Dark Matter no one has been able to detect it directly. However there is still compelling evidence supporting Dark Matter. One piece of evidence of Dark Matter is that even though we cannot observe Dark Matter directly, we can see its effect in the rotation of galaxies. This is because Dark Matter interacts gravitationally with visible matter.

There are a lot of theories of how Dark Matter particles might couple to the Standard Model, which is the model that describes all known particles and interactions that have been discovered so far. One of them is the subject of this thesis, namely a model where two new bosons are introduced, one spin-1 boson called the Z' boson, and a spin-0 scalar boson called the Dark Higgs (s).

The gauge boson Z' comes from a new gauge symmetry group $U(1)'$ which has been predicted by several theories and arises as a natural extension of the Standard Model [2]. One example of a theory that makes this prediction is the Grand Unified Theory [3].

The Dark Higgs arises naturally by assuming that the Dark Matter particles masses are generated in the same manner as the particle in the Standard Model i.e via a Dark Higgs mechanism. Having a Dark Higgs boson would also help in the search for Dark Matter, due to the possibility of the Dark Higgs being a lighter state in the dark sector compared to the Dark Matter particles. Having this lighter state in the dark sector means that it will no longer be necessary for the Dark Matter particles to couple directly to the Standard Model. Instead, the Dark Higgs can couple to the Standard Model. Thus the constrictions following from the relic abundance of the Dark Matter will be relaxed. Relic abundance is a measurement of the present remaining particles from the early universe, a more detailed explanation can be seen in section 2.3.1.

This thesis studies a possible signal of such a Dark Higgs, and the signal efficiency compared to Dark Matter searches using the Standard Model Higgs. This has been done by reimplementing an ATLAS search for Dark Matter produced together with a Standard Model Higgs[4], which decays into $b\bar{b}$ called *mono* – $H \rightarrow b\bar{b}$ search [4].

2 Theory and Motivation

2.1 Standard Model

The Standard Model of particle physics describes all the known elementary particles and interactions. These particles can be divided into two main groups: fermions and bosons, which then can be divided into several sub-groups.

Fermions are the particles which make up all known matter and have a spin value of 1/2. These particles can be divided into two groups, leptons and quarks.

Leptons can either be neutral or have a charge, the charged leptons are the electron (e), the muon (μ) and the tau (τ). Each of these have a charge of $-1e$, which means that they have one electric charge of one electron. The neutral leptons are the neutrinos, where

each neutrino is associated with a specific charged lepton. Thus the names of the different neutrinos are, the electron neutrino ν_e , the muon neutrino ν_μ and the tau neutrino ν_τ .

Quarks are particles which make up hadrons, like the protons. As for the leptons, quarks also have an electric charge but their charge is either $-1/3e$ or $+2/3e$. The quarks also have an additional charge called color charge, which can be red, blue or green. Due to the color charge of the quarks and the special properties of the strong interaction, the quarks are unable to exist in a non-bound state, i.e, they can only exist inside hadrons, which is known as color confinement. The Standard Model contains six quarks, up u , down d , strange s , charm c , top t and bottom b .

Fermions also have a corresponding anti-particle, that has the same properties as the particle, but with opposite additive quantum numbers. Table 1 shows an overview of the fermions and their corresponding anti-particles.

Table 1: Overview of all fermions and their corresponding anti-particles of the Standard Model.

Type of Fermion	Notation	Anti-particle	Electric charge (anti-particle charge)	Color multiplicity
Up-type quark	u	\bar{u}	$+2/3$ ($-2/3e$)	3
	c	\bar{c}		
	t	\bar{t}		
Down-type quark	d	\bar{d}	$-1/3e$ ($+1/3e$)	3
	s	\bar{s}		
	b	\bar{b}		
Charged lepton	e	e^+	$-1e$ ($+1e$)	-
	μ	μ^+		
	τ	τ^+		
Neutral lepton (neutrino)	ν_e	$\bar{\nu}_e$	0	-
	ν_μ	$\bar{\nu}_\mu$		
	ν_τ	$\bar{\nu}_\tau$		

The second group of elementary particles are the bosons. Bosons come in two different groups: the gauge bosons which have the spin value of 1 and, scalar bosons. So far only one scalar boson has been discovered, the Higgs boson, which will be described in more detail in section 2.2.

The gauge bosons are known as force carrying particles, as they mediate interactions between particles. The gauge bosons are the photon (γ), W^\pm , the Z^0 and the gluon (g). The force which the different gauge bosons mediate, their charge, mass and with which type of particles they interact with can be seen in table 2.

Table 2: All known gauge bosons and their mass, charge and with which particles they interact with. The mass values can be found at <http://pdg.lbl.gov/>.

Particlen	mass [GeV]	charge	Interaction	Interacts with
γ	0	-	Electromagnetic	particles which carry an electric charge
g	0	2 color charges	strong	quarks, gluons
W^\pm	80.380 ± 0.015	$\pm 1e$	weak	leptons, quarks
Z^0	91.1876 ± 0.002	0	weak	leptons, quarks

2.2 Higgs

Mass is one of the most fundamental properties of particles, and back in the early 1960s physicists were still unable to explain how particles acquire their mass. However in 1964[5, 6, 7] three theoretical physicists developed a mathematical formalism which describes how fundamental particles acquire mass. The formalism is named the Brout-Englert-Higgs mechanism after the physicists who came up with it.

In the following sections there will be a brief description of the Brout-Englert-Higgs mechanism, the Brout-Englert-Higgs field and the Higgs boson.

2.2.1 Brout-Englert-Higgs mechanism

The introduction of the electroweak force, which is the combination of the electromagnetic and the weak force, had a problem. The equations describing the electroweak force produced four bosons, which is as it should. However, all these bosons came out massless, and did not correspond to the bosons of the electroweak force where three of the particles have mass.

By applying the Brout-Englert-Higgs mechanism to the equations, the same as before happens, four bosons come out of the equations. However, this time not all particles are massless, in fact three of the particles become massive and one remains massless. These bosons correspond to the W^\pm , Z^0 and γ respectively.

The way the Brout-Englert-Higgs mechanism works is by providing a way to rearrange the initial equations by the introduction of a small piece of equation which corresponds to a new scalar field. Thus the Brout-Englert-Higgs mechanism breaks the symmetry, known as spontaneous symmetry breaking, making the equations locally gauge invariant.

2.2.2 The Brout-Englert-Higgs field

The corresponding field that arises due to the Brout-Englert-Higgs mechanism is called the Brout-Englert-Higgs field. It is this field that is responsible for generating the fundamental particle masses.

There are a few key differences that separate the Brout-Englert-Higgs field from other fields, for example, a magnetic field. The Brout-Englert-Higgs field does not have a source which generates it, nor does it have a vacuum expectation value of zero. It is also thought to have appeared just after the Big Bang.

If there were no Brout-Englert-Higgs field, all fundamental particles would act as the photon, i.e, move at the speed of light. However, with the Brout-Englert-Higgs field some particles are slowed down and acquire mass. The reason why slowing the particles down correlates to giving the particles mass is due to conservation of energy. As the Brout-Englert-Higgs field slows down the particles without reducing the particles energy, the energy has to go somewhere. Einstein's equation $E = mc^2$ shows that energy can be converted into mass and vice versa. Thus the particles kinetic energy can be converted into potential energy in the form of mass.

Therefore, the more a particle interacts with the Brout-Englert-Higgs field, the more mass the particle acquires.

2.2.3 Higgs Boson

The Higgs boson, which is the excitation of the Brout-Englert-Higgs field, has had a huge impact on particle physics and its discovery [8] resulted in the 2013 Nobel prize in physics. The reason for this impact is that its discovery provides the proof of the Brout-Englert-Higgs field and the Brout-Englert-Higgs mechanism.

The mass of the Higgs boson has been measured to be $m_h = 125.09 \pm 0.24 \text{ GeV}$ [9]. As can be seen in figure 1, there are several different decay channels for this mass. The channel where the Higgs boson was discovered was the $h \rightarrow \gamma\gamma$ due to the specific experimental signature of the two resulting photons. However, the branching ratio of this decay is rather small and thus it is not an efficient channel for searches of physics beyond SM. Instead the preferred channel is the $h \rightarrow b\bar{b}$, which has the highest branching ratio of $Br = 57\%$ [4], which also is the focus of this thesis, but instead of the Standard Model Higgs the Dark Higgs is used. However, for the Dark Higgs it is not necessarily that it is the $b\bar{b}$ decay that has the highest branching ratio. For a Dark Higgs mass above $\approx 140 \text{ GeV}$ it will be the WW decay that has the highest branching ratio.

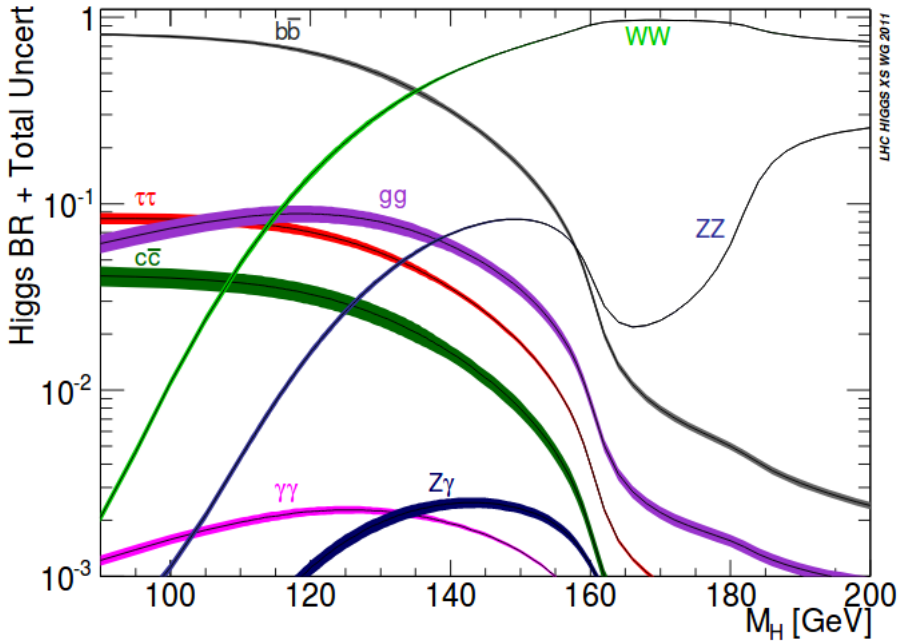


Figure 1: Branching ratio for different Higgs boson masses. The thickness of the lines indicates the uncertainty [10].

2.3 Beyond the Standard Model

2.3.1 Dark Matter

The concept of Dark Matter comes from observations in astrophysics and cosmology regarding the rotations of the galaxies. As it turns out, the stars in the outer part of the galaxies rotate at a velocity greater than can be explained with physics, as the gravitational force would be too weak. From this physicists proposed that there must be more mass in galaxies than what can be observed. Thus Dark Matter was introduced, which is a type of invisible matter that only interacts with visible matter via the gravitational force. Therefore it is only the effect of Dark Matter which has been observed, and not the matter itself.

Relic abundance is the amount of matter that is left after the freeze out. In the early universe when it was hot enough to achieve thermal equilibrium, Dark Matter particles were constantly annihilating into Standard Model Particles and vice versa. However, as the universe expanded and cooled down, the Dark Matter particles interaction rate got lower until it reached the expansion rate which is called freeze out. After this moment the Dark Matter particles density is too low compared to the interaction strength, and the amount of Dark Matter particles stays the same. In the graph in figure 2 the freeze out is at the point where the dashed line meet the solid line.

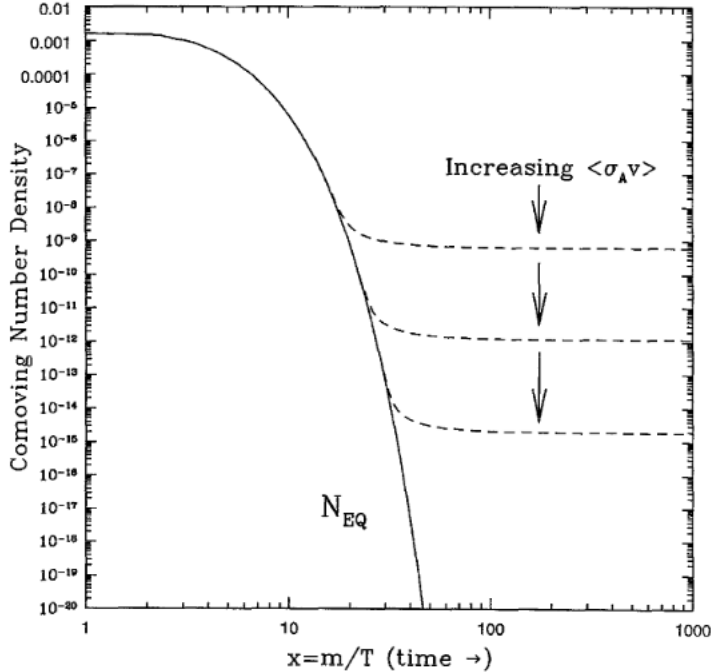


Figure 2: Figure shows the comoving number density of a WIMP (Weakly Interacting Massive Particle), where the solid line represents the the thermal equilibrium abundance and the dashed lines are the actual abundance. From [11]

There are several theories regarding different types of Dark Matter particles. However, so far the most popular theory is the WIMP (Weakly Interacting Massive Particles) theory. The reason why the WIMP theory is so popular is due to the flexibility of the theory, its large mass range of 10 GeV - 10 TeV and an expected interaction cross section which puts the WIMPs in a region that is well discoverable at the LHC.

At the moment of writing there have only been indirect observations of Dark Matter, and not any direct observation of it, although there are several different types of experiments and techniques created for the purpose of trying to discover Dark Matter.

At particle accelerator facilities, such as the LHC (Large Hadron Collider), physicist are trying to discover Dark Matter by colliding two protons, and if the collision has high enough energy there can be a pair production of two Dark Matter particles. Since the detectors can not detect the Dark Matter particles, the resulting events will have a large amount of missing transverse momentum (E_T^{miss}). E_T^{miss} is defined as $\sum_i p_T(i)$ where i is the individual particles and p_T (transverse momentum) is the momentum perpendicular to the beam axis.

2.3.2 Dark Higgs

Measurements of the Standard Model Higgs boson production and decays [12] result in strong constraints of the parameter space in which the Dark Matter particles can receive their relic abundance from annihilation into Standard Model states. However, by introducing a new state which is lighter than the Dark Matter particles, the constraints will be relaxed due to the new annihilation channel.

Introducing a new type of Higgs field in the dark sector, namely a Dark Higgs field, can provide this lighter state in the form of the Dark Higgs boson. Adding a Dark Higgs field will also come natural by assuming that the Dark Matter particles acquire their mass in the same manner as the Standard Model particles. If the new Dark Higgs boson is a lighter state than the Dark Matter particles, the relic abundance would be dominated by Dark Matter particles annihilating into two Dark Higgs bosons, which then can decay into Standard Model states.

Thus the relic density will only depend on the coupling between the Dark Higgs and the Dark Matter particles. The coupling between the Standard Model and the Dark Higgs can be very small, since the relic abundance of Dark Matter particles is stable.

By using these criteria the observed relic abundance of Dark Matter can be recreated [13, 14]. To see a formal motivation and calculations of this theory see the article *Hunting the dark Higgs*[15].

This thesis will focus on the decay where a Z' recoils against a visibly decaying Dark Higgs (s). After this interaction the Z' will decay into two Dark Matter particles and the s will decay into one bottom quark, and one anti-bottom quark as can be seen in figure 3.

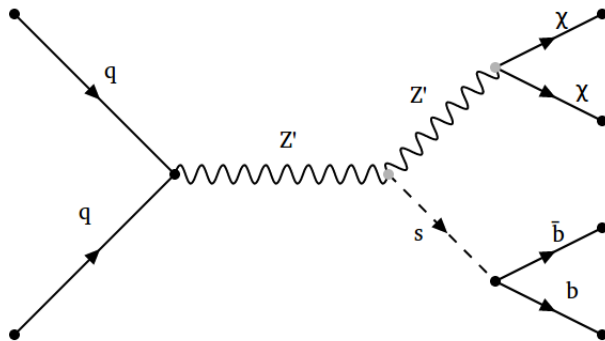


Figure 3: Feynman diagram showing the interactions of a visibly decaying Dark Higgs (s) and the boson Z' , where the Z' decays into two dark matter particles (χ) and s decays into two Standard Model bottom quarks (b, \bar{b}).

In cases where there is a high amount of missing transverse momentum ($E_t^{miss} > 500$ GeV), the Dark Higgs will be highly boosted. In such a case the experimental signature created by the decay seen in figure 3 will be one large-R jet (fat jet) made up of 2 collimated b-jets¹. The radius R is given by $R = \sqrt{(\Delta\eta)^2 + (\Delta\phi)^2}$, where $\Delta\eta$ is the difference in pseudorapidity and $\Delta\phi$ is the difference in azimuthal angle.

3 LHC

The LHC is a 27km long circular particle accelerator based at CERN, Geneva, Switzerland. This makes it the longest particle accelerator in the world, it is also the particle accelerator

¹b-jets are jets originating from bottom quarks.

which has the highest energy and luminosity (at the time of writing).

There are three types of collisions that take place at the LHC, these are: p-p (proton-proton) collisions, Pb-p (lead-proton) collisions and Pb-Pb (lead-lead) collisions.

The LHC has four large main experiments and three smaller ones. The main experiments are: ATLAS (A Toroidal LHC ApparatuS), ALICE (A Large Ion Collider Experiment), CMS (Compact Muon Solenoid) and LHCb (LHC-beauty). Both ATLAS and CMS are general purpose detectors, while ALICE and LHCb are designed for specific purposes. The smaller experiments are: TOTEM (Total Cross Section, Elastic Scattering and Diffraction Dissociation), LHCf (LHC-forward) and MoEDAL (Monopole and Exotics Detector At the LHC).

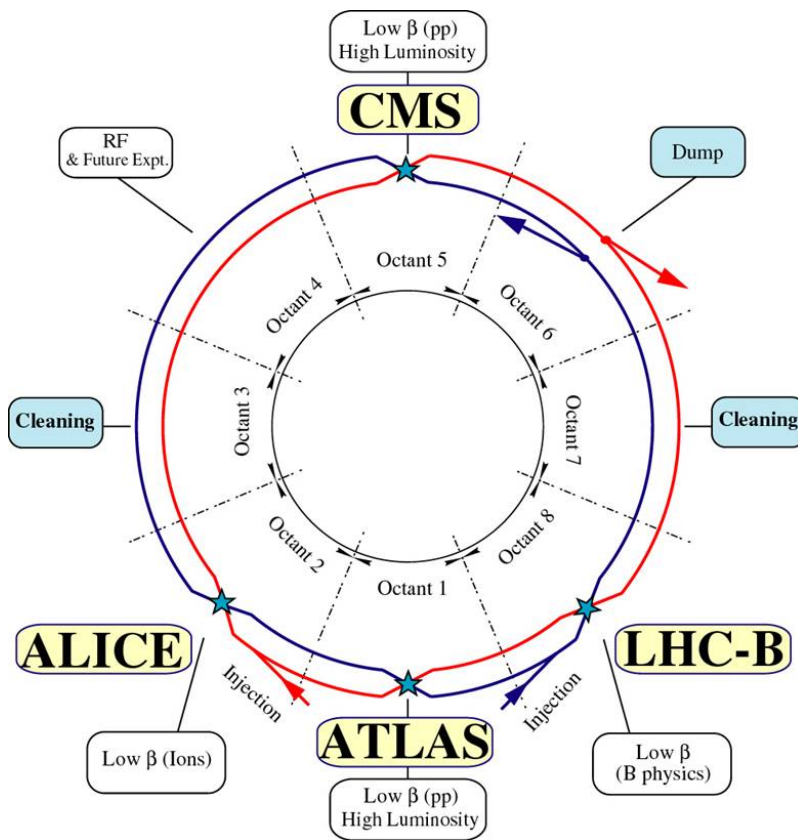


Figure 4: Schematic of the placement of the four main experiments at LHC (https://lhc-machine-outreach.web.cern.ch/lhc-machine-outreach/lhc_in_pictures.htm)

4 ATLAS

The ATLAS detector [16] (see figure 5) is a cylindric particle detector built up of several different layers, with each layer serving a specific purpose. The main components are the inner detector (ID)[17], the calorimeters[18] and the muon spectrometer[19].

ID: The ID, which is also known as the tracking system, is used to determine the direction, momentum and the charge of the particles produced in the collision. To do this the ID is constructed of three main components: a pixel detector, semiconductor tracker and a

Transition Radiation Tracker. All of these components are also immersed in a 2T strong magnetic field generated by a solenoid magnet.

Calorimeters: The task of the calorimeters is to measure the energy of the different particles via total absorption. The electromagnetic calorimeters "absorb" the electrons and photons via electromagnetic interactions. The hadron calorimeters "absorb" the energy of hadrons via the strong nuclear force.

Muon spectrometer: The muons do not interact with the calorimeter as other particles. Thus the most outer part of the detector is a muon spectrometer. This is used as another tracking system which determines the charge, momentum and direction of the passing muons.

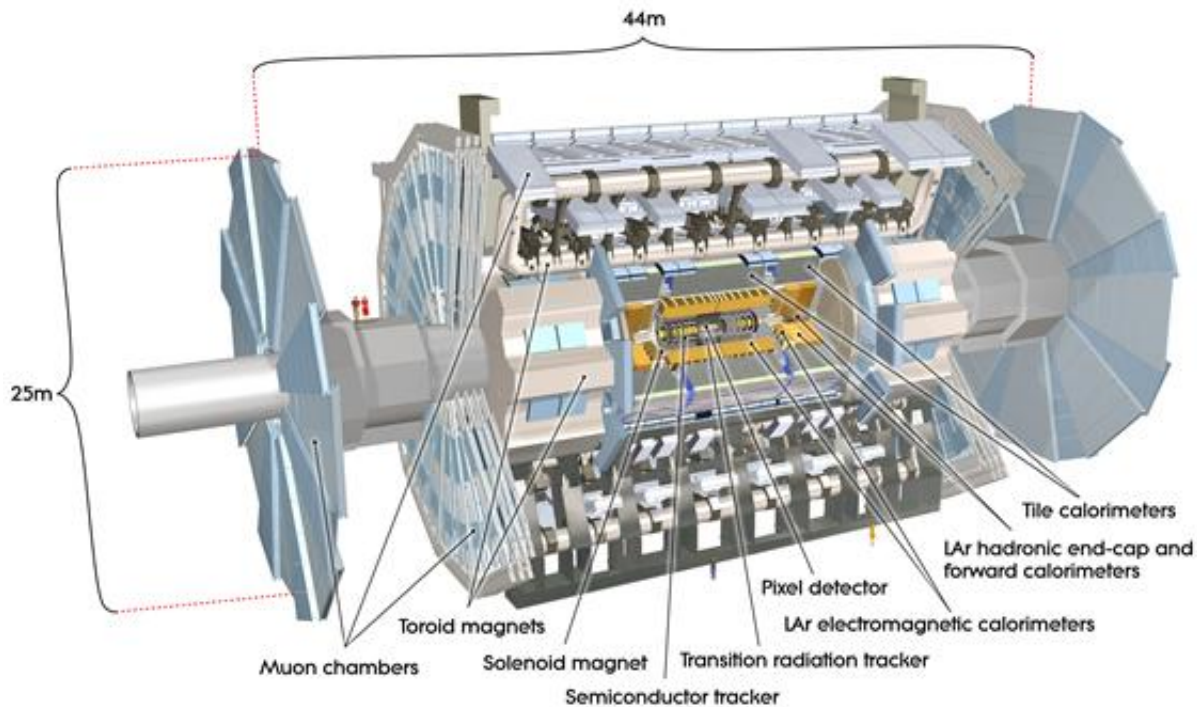


Figure 5: Figure shows a cross section illustration of the ATLAS detector. From <https://atlas.cern/discover/detector>

5 Analysis

The analysis which is based on a previous ATLAS analysis [4] was implemented in **Rivet version 2.5.4** [20], then the analysis was used on a set of signal samples. The masses of the Dark Higgs, the Z' and the DM particles were specified in these signal samples. The way the analysis was implemented can be seen in the following sections, as well as the parameter of the different jet type and the selection cuts used.

As mentioned in previous sections, the decay of the dark Higgs results in a pair of bottom quarks, which if the dark Higgs is highly boosted ($E_T^{miss} > 500$ GeV) merge into a large-R jet. Thus our approach for this analysis is based on the same technique as used in the search for Dark Matter using the Standard Model Higgs boson [4].

5.1 Jets

In total three types of jets were used in this analysis, where the different jets have to full fill different criteria, see table 3. The criteria for the different jets can be found in more detail in [4]. The clustering of the jets is done with the anti- k_t algorithm [21].

For the reconstruction of the large-R jets the class **Fastjets** [22] was used. The radius parameter of the Large-R jets was set to $R = 1$ and the jet was required to have a transverse momentum $p_T > 200$ GeV and $|\eta| < 2.0$.

To identify the large-R jets containing bottom quarks which would be the dark Higgs candidates, track-jets were used. The track-jets had a radius parameter $R = 0.2$ with the requirement of a transverse momentum $p_T > 10$ GeV and $|\eta| < 2.5$. If they contain bottom quarks, they also have to be associated to the large-R jet, i.e have a $\Delta R < 1$.

Having an event with a large-R jet fulfilling the criteria mentioned above is not enough. There also has to be a large amount of missing transverse momentum $E_T^{miss} > 500$ GeV, however, as it will be seen in the result section, that is not always the case.

Table 3: The selection of the different types of jets in the analysis, the backslash in the table represents "or" for the jets that have several different criteria.

Jet type	Transverse momentum (P_T)	Rapidity(η)
Large-R jet	$P_T > 200\text{GeV}$	$ \eta < 2.0$
Small-R jet	$P_T > 20\text{GeV}$ \ / $P_T > 30\text{GeV}$	$ \eta < 2.5$ \ / $2.5 < \eta < 4.5$
Track jet	$P_T > 10\text{GeV}$	$ \eta < 2.5$

5.2 Selection cuts

The analysis uses the same selection cuts for the merged region² as in paper [4], which the analysis is based on, in order to be able to compare the efficiencies. The exact selection cuts used can be seen in table 4. In this section there will also be a short motivation for each cut and reasoning why some cuts were excluded in the analysis. Before these cuts were implemented there were already some cuts made on the jets which can be seen in section 5.1.

²merged region means that it is the signal region for two b-jets that merge into one fat jet.

Table 4: table of all selection cuts implemented in the analysis.

Selection cut
$E_T^{miss} > 500 \text{ GeV}$
$p_T^{miss,trk} > 30 \text{ GeV}$
$\min \left[\Delta\phi(E_T^{\vec{miss}}, p_T^{\vec{j}}) \right] > \pi/9$
$\Delta\phi(E_T^{\vec{miss}}, p_T^{miss,trk}) < \pi/2$
$N_J \geq 1$
τ Veto
$b - jet$ Veto
$H_T - Ratiocut(0.57)$
$50 < m_{s,reco}/\text{GeV} < 270$
$N(b - tags) = 2$
$N(b - tags) = 1$

- $\underline{E_T^{miss} > 500\text{GeV}}$: A high amount of missing transverse momentum ensures the production of a highly boosted dark Higgs resulting in two collimated b-quarks which merge into a large-R jet. The missing transverse transverse momentum were reconstructed in the same manner as in [4], where the missing momentum is the negative of the visible finale state particles transverse momentum.
- $\underline{p_T^{miss,trk} > 30\text{GeV}}$: This cut is used to suppress background, thus it was excluded from the analysis, since there was no background in our simulation.
- $\underline{\min \left[\Delta\phi(E_T^{\vec{miss}}, p_T^{\vec{j}}) \right] > \pi/9}$: This cut is there in case there are multi-jets, where one jet is in the same direction as the $E_T^{\vec{miss}}$, which happens if a jet is mis-measured. This cut is only applied for the first three leading jets.
- $\underline{\Delta\phi(E_T^{\vec{miss}}, p_T^{miss,trk}) < \pi/2}$: This cut was excluded both because it is used to reduce background and since $p_T^{miss,trk}$ was not used.
- $\underline{N_J(\text{Nummber of fat jets}) \geq 1}$: This cut makes sure that there is at least one fat jet in the event, since the leading fat jet is the signature of the Dark Higgs decay.
- $\underline{\tau}$ Veto: Due to no τ in the simulation, this cut was excluded from the analysis
- $\underline{b - jet}$ Veto: Removes all events which contain jets from b-quarks not associated to the large-R jet, due to the risk of a t -quark decaying into bottom.

- $H_T - \text{Ratiocut}$ (0.57): The $H_T - \text{Ratio}$ is given by: $\frac{\sum p_T(\text{non-associated jets})}{\sum p_T(\text{non-associated jets}) + \sum p_T(\text{leading fat jet})}$, where the non-associated jets are defined as $\Delta R(\text{jet}, \text{leading fat jet}) > 1$. The cut is used in order to reduce background events from $t\bar{t}$.
- $50 < m_{s, \text{reco}}/\text{GeV} < 270$: This cut ensures that the signal corresponds to the Dark Higgs mass and nothing else.
- $N(b - \text{tags}) = 2$: This cut is used to select the two b-jets which is the result from the Dark Higgs decay.
- $N(b - \text{tags}) = 1$: In events with $E_T^{\text{miss}} \gg 500$ GeV the two b-jets have a risk of "blending" together, thus it can appear as if there is only one b-jet.

5.3 b-tagging

b-tagging is an important method used in particle physics, due to the unique jet formation. It is also an especially important method when it comes to studying the Higgs, since the Higgs most commonly decays into two b-quarks. The reason why it is possible to b-tag a jet is because the B-hadron that is created from the b-quark decays quickly, resulting in a second vertex. It is this second vertex which the tagging algorithms uses in order to identify the b-jets.

For the b-tagging of the jets in this analysis, one of Rivet's built-in functions called *containsBottom* () [20] was used. This function checks whether the selected jets contain any hadron which has bottom quarks. For this analysis b-tagging was used to make sure that there were only bottom quarks in the fat jet and the associated track-jets. This is due to the decay of the Dark Higgs into two bottom quarks, thus the large-R jet containing two bottom quarks will be the result of the Dark Higgs decay. Events that contain more than two bottom quarks and/or have other jets containing bottom quarks are vetoed, by using the same function.

5.4 Signal-sample

The signal samples that have been used for this analysis have been based on the model from the article *Hunting the Dark Higgs* [15]. They were created with **Madgraph version 2.5.5** [23], **LHAPDF-6.1.6** [24] and parton showering and hadronisation with **Pythia 8** [25] at truth level³. All samples that were used had the same interactions, couplings and Z' mass. The parameters that were used were two different DM particle masses at 500 GeV and 700 GeV, with the dark Higgs masses of 90 GeV, 125 GeV, 150 GeV, 200 GeV and 125 GeV, 200 GeV respectively.

³Truth level is simulations where there are no simulated detectors i.e the information comes directly from the event generator.

6 Results

In this section the results and generated plots will be shown and discussed. All signal samples used to generate the result of this section have the same mass for Z' , which is $m'_{Z'} = 2$ TeV. The layout of the plots shows on the top the distribution of the different model parameters in different colors, in the bottom the ratio between the model parameters of the red line and the other lines can be seen, and the yellow band is the statistical uncertainty of the red line.

In the plots displayed in figures 6a, 6b it can be seen that the majority of the events has a missing transverse momentum below our cut ($E_T^{miss} > 500$ GeV), and thus the majority of Dark Higgs produced in the signal sample will not be boosted enough to create two collimated b-jets. The effect this has in the analysis is that the efficiencies are rather low compared to efficiencies for the model in the original ATLAS analysis. For both the plot with a DM mass of 500 GeV (figure 6a) and 700 GeV (6b), a clear trend can be seen by looking at the ratio between the model parameters.

The trend that can be seen is that the ratio increases as the missing transverse momentum increases. This is due to the nature of the process shown in the Feynman diagram in figure 3, since the Z' recoils against the Dark Higgs. Thus the higher the Dark Higgs mass is, the "harder" the recoil will become, which results in the DM particles having more momentum, thus there will be more missing momentum in the seen event.

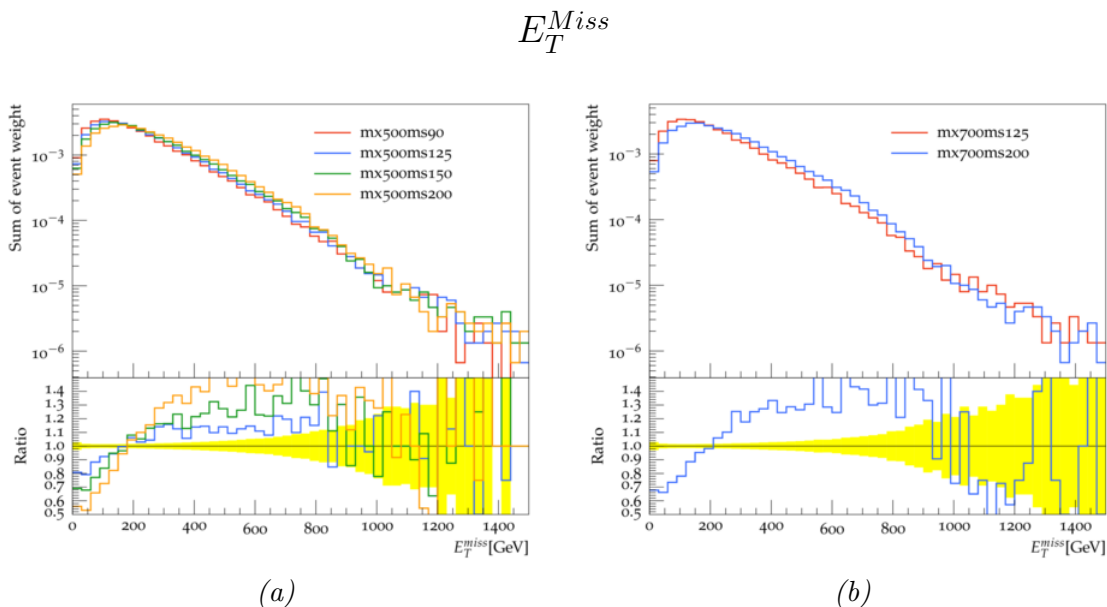


Figure 6: The figure shows the missing transverse momentum for two different DM particle masses. In figure 6a the mass of the DM particle is 500 GeV, and four different mass values for the Dark Higgs 90 GeV (red), 125 GeV (blue), 150 GeV (green) and 200 GeV (yellow). Figure 6b has DM particle mass of 700 GeV and two different mass values for the Dark Higgs are 125 GeV (red) and 200 GeV (blue).

Comparing the missing transverse momentum of the different DM particle masses (figure 7) of 500 GeV vs 700 GeV at two different dark Higgs masses 125 GeV (figure 7a) and 200 GeV (figure 7b), it can be seen that there is a trend in both figure 7a and 7b where the lighter

Dark Matter particles have a maximum at a higher missing transverse momentum value.

Comparison of E_T^{Miss} between DM mass of 500 GeV vs 700 GeV

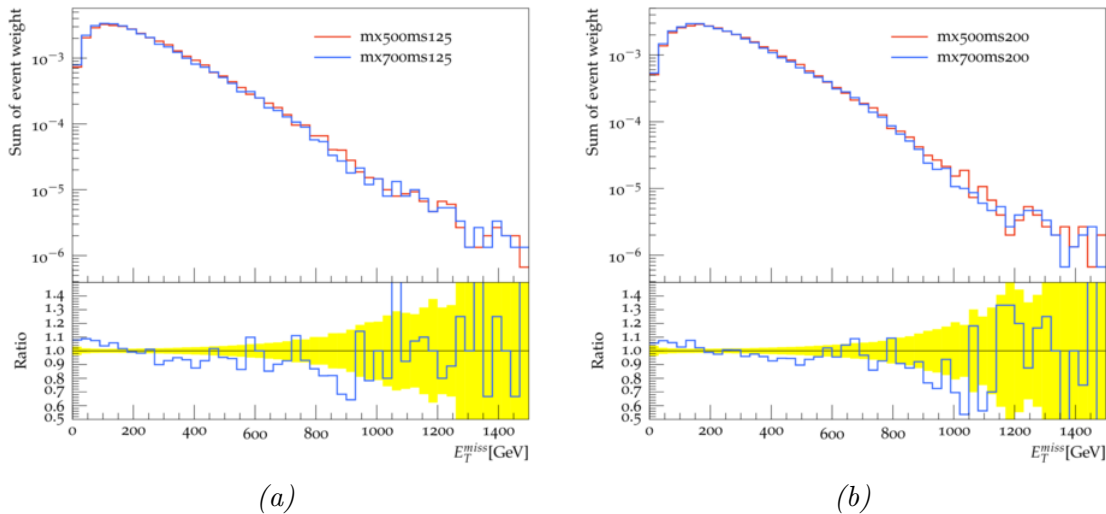


Figure 7: These plots show the comparison between the two different DM particles masses of 500 GeV (red) and 700 GeV (blue). Figure 7a shows the comparison with a Dark Higgs mass of 125 GeV and figure 7b is for a Dark Higgs of 200 GeV.

One important aspect of this project is to be able to reconstruct the mass of the Dark Higgs from the jets. This has been done in two ways: Taking the invariant mass of the leading⁴ fat jet (figure 8) and taking the invariant mass of the dijet system formed by the leading and sub-leading⁵ b-jet (figure 9).

The invariant mass for the leading fat jet which can be seen in figure 8 displays a behavior as would be expected for both DM particles mass values, by having an almost symmetrical peak at the mass value of the different Dark Higgs masses. Looking at figures 8a and 8c, which display the invariant mass of the leading fat jet without any cuts applied for DM masses 500 GeV and 700 GeV, respectively, it can be seen that there is an increase towards lower masses for each Dark Higgs mass. The reason for the increase is because since there are no cuts applied, the leading fat jet is likely to only consist of one b-jet.

However, by looking at figures 8b and 8d, which display the invariant mass of leading fat jet with all cuts applied, for DM particle masses of 500 GeV and 700 GeV, respectively, there is now only one peak for each of the mass values of the Dark Higgs. The peaks all have an approximately symmetrical shape with a maximum at the mass value specified in the event generation, which is as expected.

⁴The leading jet is the jet with the highest p_T .

⁵The sub-leading jet is the jet with the second highest p_T .

Invariant mass of leading fat jet

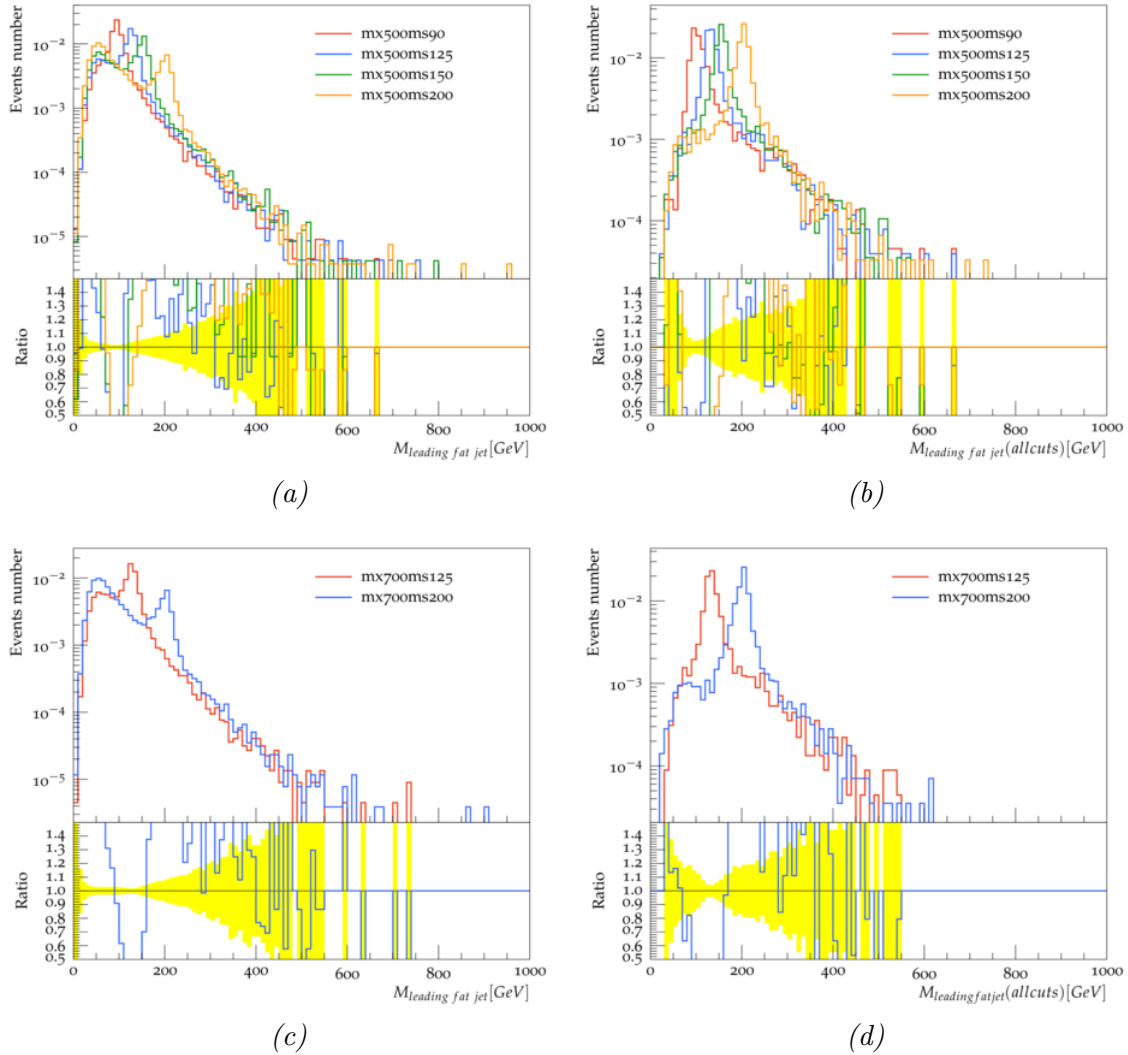


Figure 8: Plots show the invariant mass of the leading fat jet. Figures 8a (No cuts applied) and 8b (all cuts applied) shows DM particle mass of 500 GeV and Dark Higgs masses 90 GeV (red), 125 GeV (blue), 150 GeV (green) and 200 GeV (yellow), and figures 8c (No cuts applied) and 8d (all cuts applied) shows a DM particle mass of 700 GeV and Dark Higgs masses of 125 GeV (red) and 200 GeV (blue).

Looking at the invariant mass for the dijet system formed by the leading and sub-leading b-jet (figure 9) which correspond to the decay of a highly boosted Dark Higgs when all cuts are applied, the behavior of all four plots (9a,9b, 9c, 9d) is rather similar when looking at the peaks corresponding to the different mass values of the Dark Higgs. That is that all peaks display a steep fall at the corresponding mass value instead of a symmetrical distribution as the peaks for the leading fat jet. At the moment of writing the reason for this odd behavior is not understood. However, there are some possible explanations that might be able to shed some light on why this behavior is seen in the plots.

The first explanation is that the b-tagging function does not work as we think, which

might have led to the creation of a bug that results in the behavior displayed in the plots. The second one is that there is also a possibility of leptonic decays in form of neutrinos creating additional missing energy. Last explanation is that since the radius of the track-jets used is so small ($R=0.2$), it only contains the resulting particles from the b-quarks and nothing else. Thus the invariant mass will not exceed the Dark Higgs mass value, resulting in a steep fall. The small radius might also not be able to contain all of the b-jet, thus there will be a loss in energy resulting in a tail seen in the figures.

Invariant mass for the leading and sub-leading b-jets

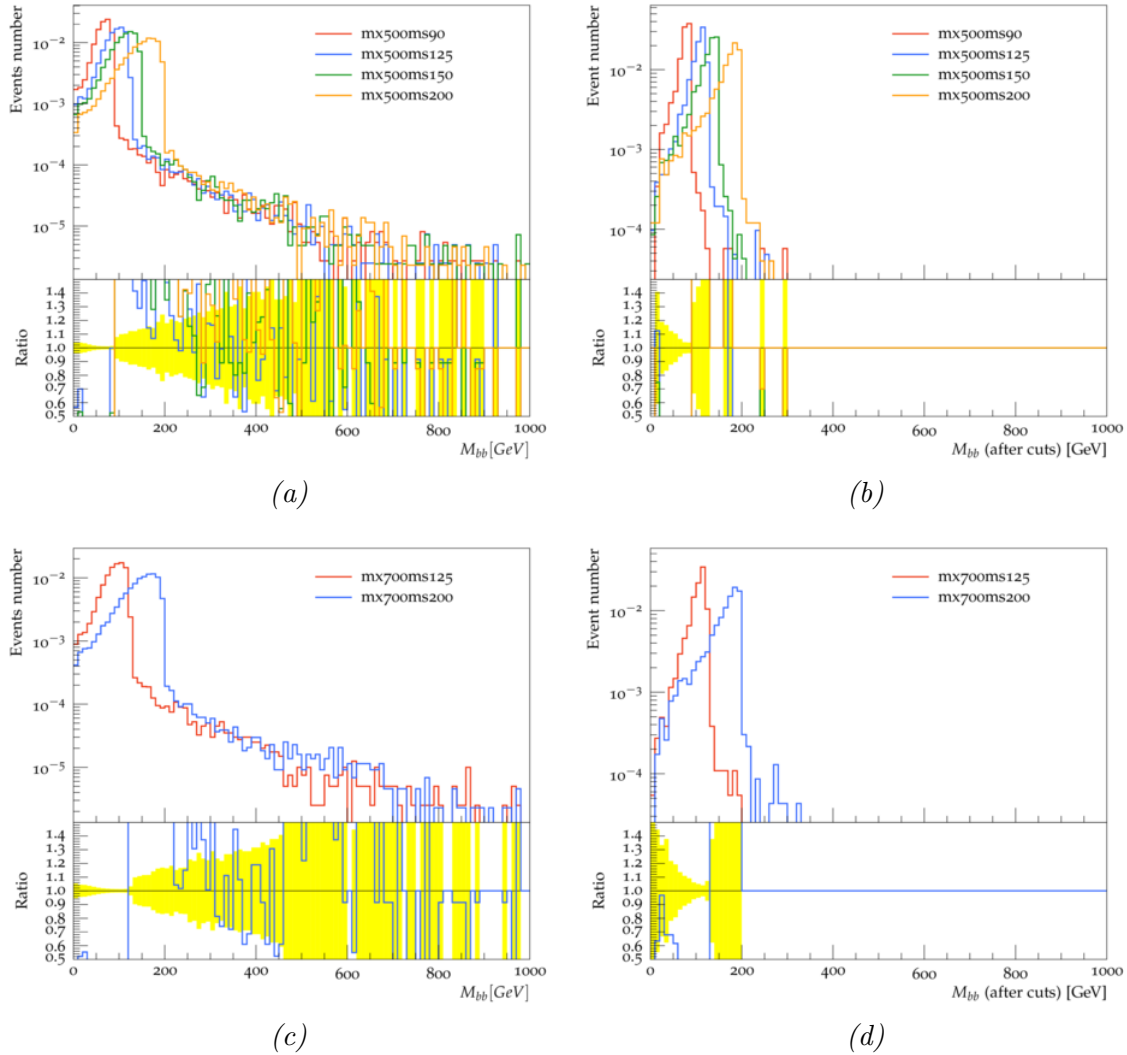


Figure 9: The figures show the invariant mass for a dijet system formed by the leading and the sub-leading b-jets. Figure 9a and 9b shows the invariant mass for the two b-jets with a DM particle mass of 500 GeV and the Dark Higgs masses 90 GeV (red), 125 GeV (blue), 150 GeV (green) and 200 GeV (yellow), with cuts (9b) and without any cuts (9a). Figure 9c and 9d shows the invariant mass for the two b-jets with a DM particle mass of 700 GeV and the Dark Higgs masses 125 GeV (red) and 200 GeV (blue), where figure 9c has no cuts applied and figure 9d is with all cuts applied.

By looking at the ΔR between the leading fat jet, leading b-jet and sub-leading b-jet, it can be seen if the b-jets actually make up the fat jet or if the fat jet is a result of something else. Figures 10a, 10c show the $\Delta R(\text{leading fat jet, leading b-jet})$ and $\Delta R(\text{leading fat jet, sub-leading b-jet})$ respectively. It can be seen that even though the main peak is within $\Delta R < 1$, there is a substantial amount of events where the b-jets are produced outside the leading fat jet. This occurs since there is no cut applied on the missing momentum, thus there are a lot of events where the Dark Higgs is not highly boosted and the two bottom quarks produced in the decay will not be collimated. This is also consistent with why there is an increase at low mass values in the plots of the invariant mass of the leading fat jet without any cuts (figures 8a and 8c).

However, by looking at the plots of $\Delta R(\text{leading fat jet, leading b-jet})$ (figure 10b) and $\Delta R(\text{leading fat jet, sub-leading b-jet})$ (figure 10d) where all cuts have been applied, there is close to zero events that have a $\Delta R > 1$ for the leading b-jet. For the sub-leading b-jet there are a few more events with $\Delta R > 1$, but not enough to have a major impact when looking at the invariant masses.

Considering the case where all cuts are applied in figures 9b, 9d, 8b, 8d, 10b, 10d), it can be concluded from figures 10b, 10d that the dijet system formed by the leading and sub-leading b-jet forms the leading fat jet. Thus it would be expected that the plots of the invariant masses would have the same shape.

$\Delta R(\text{leading fat jet, b-jet})$

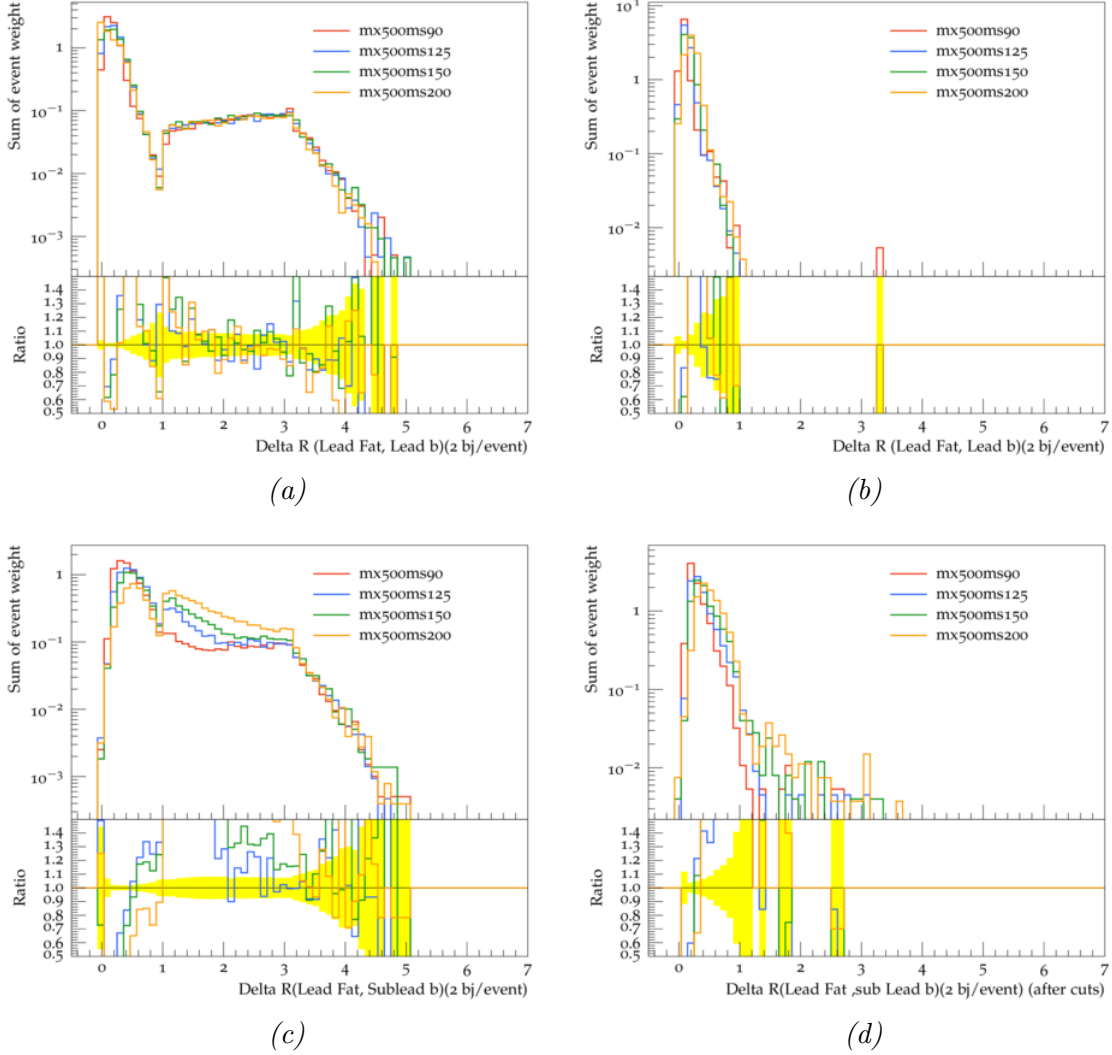


Figure 10: Figures (a) (no cuts applied) and (b) (all cuts applied) show ΔR between the leading fat jet and leading b-jet, and figures (c) (no cuts applied) and (d) (all cuts applied) show ΔR between the leading fat jet and sub-leading b-jet. For all plots the DM particle mass is 500 GeV and the Dark Higgs masses are 90 GeV (red), 125 GeV (blue), 150 GeV (green) and 200 GeV (yellow). The same plots for the DM particle mass of 700 GeV can be found in the appendix B figure 14.

In the generated events it is expected that a majority of the jets should be produced with a low η value, i.e central jets. Looking at figures 11a (no cuts applied) and 11b (all cuts applied) which display the η of the leading jet (small-R) for a DM particle mass of 500 GeV, it is clear that a majority of the events has a $|\eta| < 2.5$, which is as expected. This means that the η cuts applied to the jets should not have a major impact. More examples of η plots can be seen in appendix B figure 15.

The efficiency of the cuts for the different DM particle masses and Dark Higgs masses can be seen in table 5 (DM particle mass 500 GeV) and table 6 (DM particle mass 700 GeV). It can be seen in both tables that the first cut ($E_t^{miss} > 500\text{GeV}$) has a low efficiency, meaning

η for leading jet with and without cuts

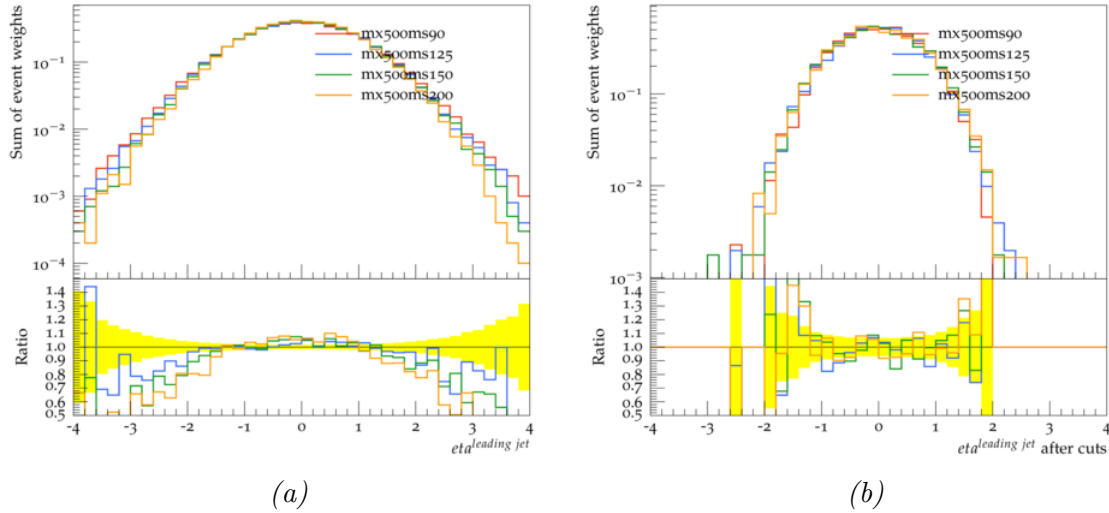


Figure 11: The plots show η for the leading jet with Dark Matter particle mass of 500 GeV, (a) is without cuts implemented and (b) is with all cuts implemented. The Dark Higgs masses are 90 GeV (red), 125 GeV (blue), 150 GeV (green) and 200 GeV (yellow). In appendix B figure 15 η for Dark Matter mass of 700 GeV can be seen.

that it removes a majority of the events. The reason for this can be seen in figure 6a and 6b, where it is clear in both figures that a majority of the events produced by the signal sample have $E_t^{miss} < 500\text{GeV}$.

One can compare the efficiencies for the signal configurations studied in this project (table 5, 6) with the efficiencies of the ATLAS mono- $H(b\bar{b})$ paper [4] seen in the table in figure 12. It is hard to make a detailed comparison since there is no 1:1 translation between the masses and other model parameters. However, the ratio from one cut to another can be studied in order to get a rough estimate of how they compare to each other, which can be seen in figure 13.

Overall, the differences in efficiencies are quite similar up to the b-jet veto cut: In our case the b-jet veto removes substantially more events comparing to the table in figure 12.

Looking at the $50 < m_{s, reco}/\text{GeV} < 270$ cut it is clear that in our analysis it does not remove any events after the $H_T - \text{Ratiocut}(0.57)$ cuts, while in figure 12 the $50 < m_{s, reco}/\text{GeV} < 270$ cut removes a significant amount of events for both (b) and (c).

The other major difference is in the $N(b - tag)$ cut. In tables 5 and 6 the $N(b - tag) = 1$ reduces the number of events by a factor of 10, which is a lot more than in the table in figure 12 both column (b) and (c). For $N(b - tag) = 2$ it can be seen in figure 13 that the ratio in our case is substantially higher.

Looking at figure 13 and as has been explained above, the major differences arises when some form of b-tagging is involved in the cut. The reason for this is most likely due to the different methods used for the b-tagging. The ATLAS paper used a method based on the second vertex, while we used the Rivet function `containsbottom()` which looks for B-hadrons in the jets, as can be read about in section 5.3.

Comparing our different signal configurations to each other, it can be seen in figure 13 that the ratio from one cut to another is similar. The biggest differences are in the ratio number 2 $\left(\frac{N_{J \geq 1}}{\min[\Delta\phi(E_T^{\vec{miss}}, \vec{p}_T^j)] > \pi/9} \right)$ and 5 $\left(\frac{N(b\text{-tags})=1}{50 < m_{s, reco}/\text{GeV} < 270} \right)$.

Table 5: The efficiencies of the different cuts, where $a(m_s = 90 \text{ GeV})$, $b(m_s = 125 \text{ GeV})$, $c(m_s = 150 \text{ GeV})$ and $d(m_s = 200 \text{ GeV})$, all samples in this table has a DM particle mass of 500 GeV.

Selection cut	a	b	c	d
$E_T^{\vec{miss}} > 500 \text{ GeV}$	0.0686	0.07738	0.08798	0.10136
$\min[\Delta\phi(E_T^{\vec{miss}}, \vec{p}_T^j)] > \pi/9$	0.06498	0.07434	0.08408	0.09722
$N_J \geq 1$	0.06476	0.07414	0.08374	0.09702
b-jet veto	0.04420	0.05112	0.05706	0.06066
$H_T - \text{Ratiocut}(0.57)$	0.04392	0.05080	0.05674	0.06050
$50 < m_{s, reco}/\text{GeV} < 270$	0.04392	0.05080	0.05674	0.06050
$N(b - \text{tags}) = 1$	0.00566	0.00438	0.00516	0.00576
$N(b - \text{tags}) = 2$	0.03494	0.04142	0.04674	0.04994

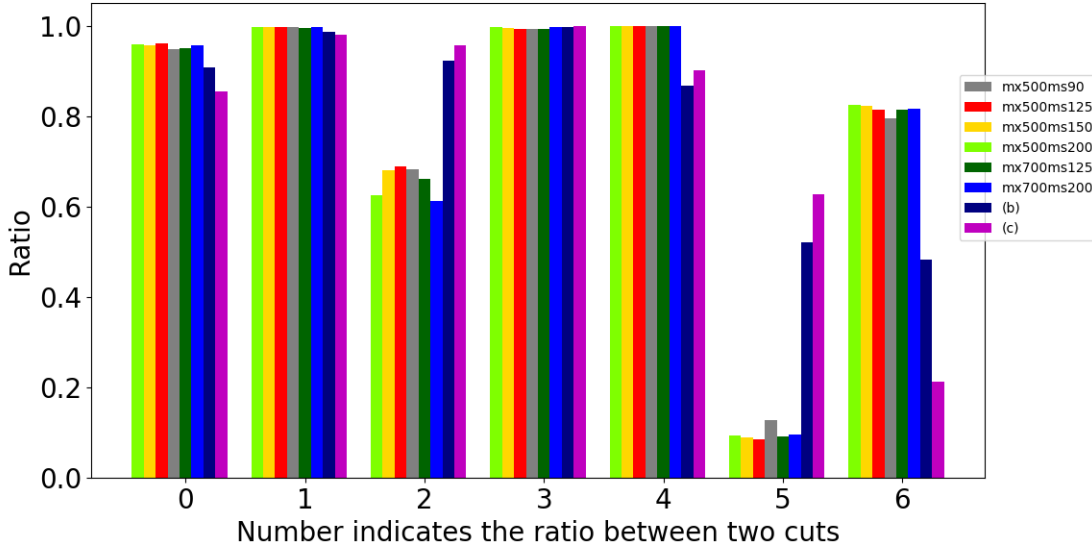
Table 6: The efficiencies of the different cuts, where $a(m_s = 125 \text{ GeV})$ and $b(m_s = 200 \text{ GeV})$ correspond to the different masses of the dark Higgs, both a and b have DM particle mass of 700 GeV

Selection cut	a	b
$E_T^{\vec{miss}} > 500 \text{ GeV}$	0.07260	0.0974
$\min[\Delta\phi(E_T^{\vec{miss}}, \vec{p}_T^j)] > \pi/9$	0.06896	0.09316
$N_J \geq 1$	0.06866	0.09280
b-jet veto	0.04534	0.05694
$H_T - \text{Ratiocut}(0.57)$	0.04502	0.05672
$50 < m_{s, reco}/\text{GeV} < 270$	0.04502	0.05672
$N(b - \text{tags}) = 1$	0.00418	0.00546
$N(b - \text{tags}) = 2$	0.03670	0.04634

Selections (merged)	(a)	(b)	(c)
$E_T^{\text{miss}} > 500 \text{ GeV}$	<0.01	0.394	0.977
$p_T^{\text{miss,trk}} > 30 \text{ GeV}$ (not for 2 b -tags)	<0.01	0.375	0.934
$\min [\Delta\phi (\vec{E}_T^{\text{miss}}, \vec{p}_T^j)] > \pi/9$	<0.01	0.358	0.834
$\Delta\phi (\vec{E}_T^{\text{miss}}, \vec{p}_T^{\text{miss,trk}}) < \pi/2$	<0.01	0.356	0.822
$N_j \geq 1$	<0.01	0.353	0.818
τ Veto	<0.01	0.343	0.798
b -jet Veto	<0.01	0.326	0.782
H_T -Ratio Cut (0.57)	<0.01	0.325	0.782
$50 < m_{h,\text{reco}}/\text{GeV} < 270$	<0.01	0.282	0.705
$N(b\text{-tags}) = 2$	<0.01	0.136	0.150
$N(b\text{-tags}) = 1$	<0.01	0.147	0.442

Figure 12: Figure/table comes from paper [4] where (a) $(m'_Z, m_A) = (0.6 \text{ TeV}, 0.3 \text{ TeV})$, (b) $(m'_Z, m_A) = (1.4 \text{ TeV}, 0.6 \text{ TeV})$, (c) $(m'_Z, m_A) = (2.6 \text{ TeV}, 0.3 \text{ TeV})$

Ratio from one cut to another



0	1	2	3
$\frac{\min \left[\Delta\phi(E_T^{\vec{m}iss}, \vec{p}_T^j) \right] > \pi/9}{E_T^{\vec{m}iss} > 500\text{GeV}}$	$\frac{N_{J \geq 1}}{\min \left[\Delta\phi(E_T^{\vec{m}iss}, \vec{p}_T^j) \right] > \pi/9}$	$\frac{b\text{-jetveto}}{N_{J \geq 1}}$	$\frac{H_T\text{-Ratiocut}(0.57)}{b\text{-jetveto}}$
4	5	6	
$\frac{50 < m_{s, reco}/\text{GeV} < 270}{H_T\text{-Ratiocut}(0.57)}$	$\frac{N(b\text{-tags})=1}{50 < m_{s, reco}/\text{GeV} < 270}$	$\frac{N(b\text{-tags})=1}{50 < m_{s, reco}/\text{GeV} < 270}$	

Figure 13: Figure displays the ratios from one cut to another, where each color represents a different signal generation and (b), (c) represent the columns (b) and (c) in figure 12. The number on the x-axis corresponds to a different ratio, which can be seen in the table below the diagram.

7 Conclusion

The concept of Dark Matter is probably one of the biggest question mark in physics of our time, due to the overwhelming evidence for its principal existence in combination with the lack of any direct observation. The reason for Dark Matter being of such importance is due to the fact that the universe consists of about 5 times more Dark Matter than regular light matter, thus to understand the universe we live in, we must understand what Dark Matter is.

At particle accelerators physicists are looking for Dark Matter in different types of decay channels, and since the discovery of the Higgs boson, the number of possible experimental signatures has increased significantly. The more decay channels there are, the larger is the chance of discovering the elusive Dark Matter particles.

The potential of a new decay channel with a Dark Higgs that decays into two bottom

quarks, which has been the focus of this thesis, would not only provide an additional search channel for Dark Matter particles, but also provide an explanation of how the Dark Matter particles acquire their mass.

Looking at the results obtained from the truth level signal samples which have been analyzed and studied in this thesis, one can conclude that the model is validated, since the results behave approximately as what would be expected. The invariant masses of the fat jet (Figures 8a, 8b, 8c, 8d) reproduce a mass peak with a symmetrical distribution corresponding to the Dark Higgs masses. However, studying the invariant mass of the two leading b-jets 9a, 9b, 9c, 9d), the plots display a rather odd behavior by having a steep fall at the mass value. The reason for the steep peak is unknown (at the moment of writing), but there are several ideas for why this behavior occurs, which will be explored in the future.

The efficiencies of the cuts are rather hard to compare to the ATLAS result, since in our analysis we used different model with different parameters and had samples which produce most events with a low amount of missing transverse momentum. However, a rough comparison can still be done, where it is clear that the major differences are in the b-jet veto, $50 < m_{s, reco}/GeV < 270$, $N(b - tags) = 1$ and $N(b - tags) = 2$ cut.

For the model parameters studied in this thesis, the analysis seems to have a potential for studying this model. However, more research has to be made before being able to say anything definite.

8 Outlook

This project will continue by first looking into why there is such a difference between the shape of the peaks in the plots for the invariant mass of the fat jets and the invariant mass of the leading b-jet and sub-leading b-jet. After this is understood, the most likely expansion of this project is to analyze more samples with more combinations of mass values for Z' , Dark Matter particles and the Dark Higgs, in order to make a more substantial analysis of the Dark Higgs model.

It has also been suggested to look into the resolved region and not just only the merged region, which has been the focus region in this thesis.

9 Acknowledgements

I first would like to thank Ruth Pöttgen for the opportunity to do this project. It has been a great learning experience and extremely interesting. I would also like to thank Ruth for all the help she has given me, both with the project itself and with the writing of this report. Overall, she has been a great supervisor and it has been a pleasure working with her.

Next, I would like to give a special thank to Eleni Skorda for all the time and effort she has put into helping me with the writing of the analysis and understanding of the physics. Without her, this thesis would not have been possible within such a short time frame.

Next, I would also like to thank Lukas Heinrich for all the help with Rivet and the signal samples.

Finally, I would like to thank everyone at the department for all the nice discussions and all the help/input during this thesis.

Bibliography

- [1] Marc Schumann. Dark matter 2013. *Brazilian Journal of Physics*, 44(5):483–493, 2014.
- [2] Oleg Lebedev and Yann Mambrini. Axial dark matter: the case for an invisible z' . *Physics Letters B*, 734:350–353, 2014.
- [3] Daniel Hayden, Raymond Brock, and Christopher Willis. Z prime: a story. *arXiv preprint arXiv:1308.5874*, 2013.
- [4] ATLAS Collaboration et al. Search for dark matter produced in association with a higgs boson decaying to $b\bar{b}$ using 36 fb^{-1} of pp collisions at $\sqrt{s} = 13\text{ tev}$ with the atlas detector. *arXiv preprint arXiv:1707.01302*, 2017.
- [5] Peter W Higgs. Broken symmetries and the masses of gauge bosons. *Physical Review Letters*, 13(16):508, 1964.
- [6] François Englert and Robert Brout. Broken symmetry and the mass of gauge vector mesons. *Physical Review Letters*, 13(9):321, 1964.
- [7] Pauline Gagnon. *Who Cares about Particle Physics?: Making Sense of the Higgs Boson, the Large Hadron Collider and CERN*. Oxford University Press, 2016.
- [8] ATLAS Collaboration et al. Observation of a new particle in the search for the standard model higgs boson with the atlas detector at the lhc. *arXiv preprint arXiv:1207.7214*, 2012.
- [9] C. Patrignani et al. Review of Particle Physics. *Chin. Phys.*, C40(10):100001, 2016.
- [10] A Denner, Sven Heinemeyer, Ivica Puljak, D Rebuzzi, M Spira, LHC Higgs Cross Section Working Group, et al. Standard model higgs-boson branching ratios with uncertainties. *The European Physical Journal C*, 71(9):1753, 2011.
- [11] EW Kolb and MS Turner. The early universe. *Front. Phys.*, Vol. 69,, 69, 1990.
- [12] ATLAS and CMS collaboration. Measurements of the higgs boson production and decay rates and constraints on its couplings from a combined atlas and cms analysis of the lhc pp collision data at $\sqrt{s} = 7$ and 8 tev . *Journal of High Energy Physics*, 2016.
- [13] Nicole F Bell, Yi Cai, and Rebecca K Leane. Dark forces in the sky: signals from z' and the dark higgs. *Journal of Cosmology and Astroparticle Physics*, 2016(08):001, 2016.
- [14] Felix Kahlhoefer, Kai Schmidt-Hoberg, Thomas Schwetz, and Stefan Vogl. Implications of unitarity and gauge invariance for simplified dark matter models. *Journal of High Energy Physics*, 2016(2):16, 2016.
- [15] Michael Duerr, Alexander Grohsjean, Felix Kahlhoefer, Bjoern Penning, Kai Schmidt-Hoberg, and Christian Schwanenberger. Hunting the dark higgs. *Journal of High Energy Physics*, 2017(4):143, 2017.

- [16] ATLAS Collaboration. The atlas experiment at the cern large hadron collider. *Journal of Instrumentation*, 3(8):S08003–S08003, 2008.
- [17] About the ATLAS inner detector. <https://atlas.cern/discover/detector/inner-detector>. Accessed: 2017-12-04.
- [18] About ATLAS calorimeter. <https://atlas.cern/discover/detector/calorimeter>. Accessed: 2017-12-04.
- [19] About ATLAS muon spectrometer. <https://atlas.cern/discover/detector/muon-spectrometer>. Accessed: 2017-12-04.
- [20] Andy Buckley, Jonathan Butterworth, David Grellscheid, Hendrik Hoeth, Leif Lönnblad, James Monk, Holger Schulz, and Frank Siegert. Rivet user manual. *Computer Physics Communications*, 184(12):2803–2819, 2013.
- [21] Matteo Cacciari, Gavin P Salam, and Gregory Soyez. The anti-kt jet clustering algorithm. *Journal of High Energy Physics*, 2008(04):063, 2008.
- [22] Matteo Cacciari, Gavin P Salam, and Gregory Soyez. Fastjet user manual. *The European Physical Journal C*, 72(3):54, 2012.
- [23] Johan Alwall, R Frederix, S Frixione, V Hirschi, Fabio Maltoni, Olivier Mattelaer, H-S Shao, T Stelzer, P Torrielli, and M Zaro. The automated computation of tree-level and next-to-leading order differential cross sections, and their matching to parton shower simulations. *Journal of High Energy Physics*, 2014(7):79, 2014.
- [24] Andy Buckley, James Ferrando, Stephen Lloyd, Karl Nordström, Ben Page, Martin Rüfenacht, Marek Schönherr, and Graeme Watt. Lhapdf6: parton density access in the lh precision era. *The European Physical Journal C*, 75(3):132, 2015.
- [25] Torbjörn Sjöstrand, Stephen Mrenna, and Peter Skands. A brief introduction to pythia 8.1. *Computer Physics Communications*, 178(11):852–867, 2008.

A Analysis code

The code can be found at GitHub repository: <https://github.com/davidmadsen/DarkHiggs>

B Additional figures

$\Delta R(\text{leading fat jet, sub-leading b-jet})$

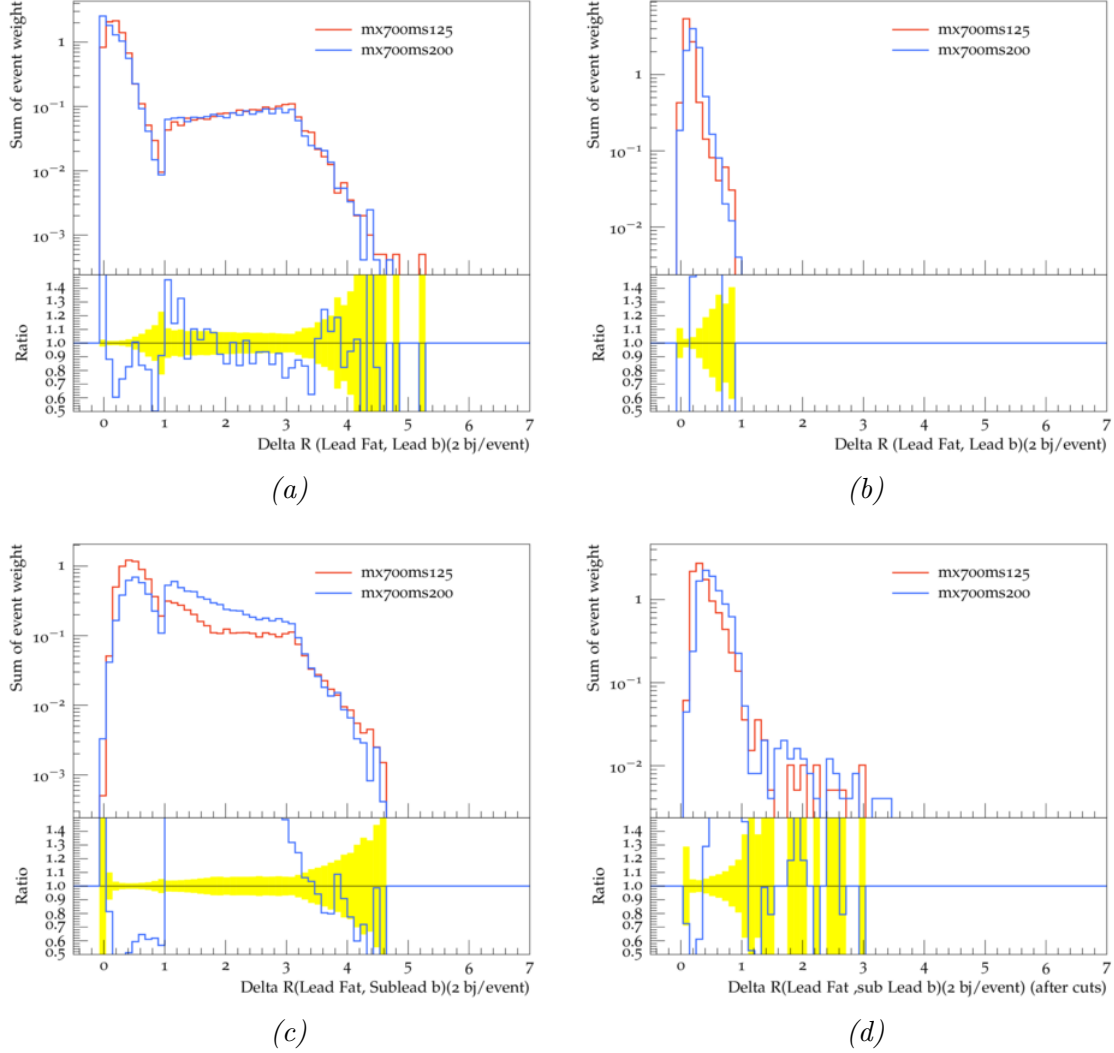


Figure 14: The Plots show the $\Delta R(\text{leading fat jet, leading b-jet})$ (a) (no cuts), (b) (all cuts) and $\Delta R(\text{leading fat jet, sub-leading b-jet})$ (c) (no cuts) and (d) (all cuts). The mass of the Dark Matter particles are 700 GeV and the dark Higgs masses are 125 GeV (red) and 200 GeV (blue).

η for leading jet with and without cuts

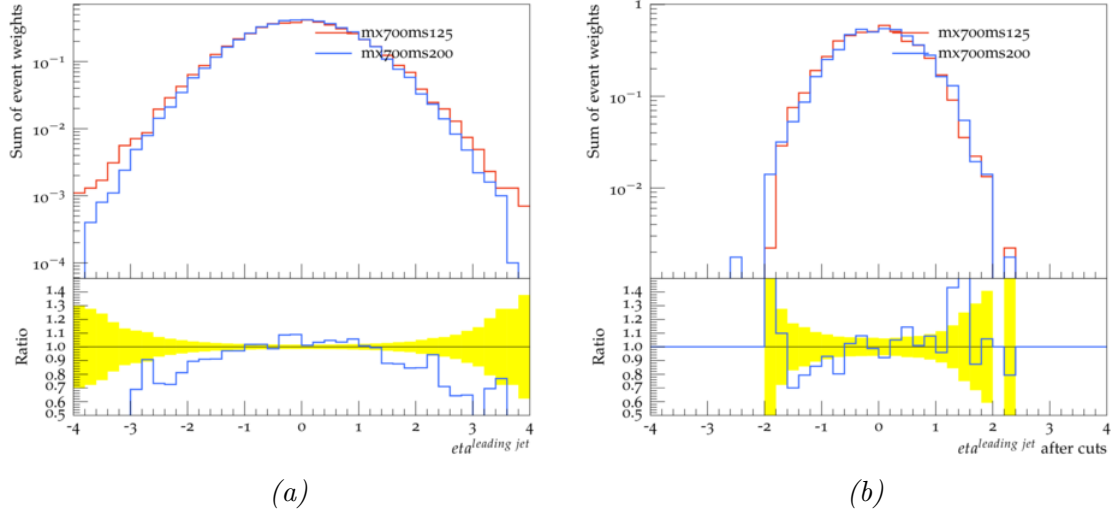


Figure 15: The plots show the η for the leading jet with the Dark Matter masses of 700 GeV and Dark Higgs masses of 125 GeV (red) and 200 GeV (blue)